European Journal of Wood and Wood Products (2024) 82:35–52
https://doi.org/10.1007/s00107-023-02002-w

ORIGINAL ARTICLE

Comparative investigation on viscoelastic and mechanosorptive creep behavior of two tropical hardwoods and one temperate softwood

Martian Asseko Ella[1] · Giacomo Goli[2] · Claude Feldman Pambou Nziengui[3] · Joseph Gril[1,4] · Eric Fournely[1] · Rostand Moutou Pitti[1,5]

Received: 28 May 2023 / Accepted: 26 September 2023 / Published online: 1 November 2023

Abstract

Two series of 3-point bending tests under constant mechanical load and temperature of 20 °C have been performed on two tropical hardwoods, *Aucoumea klaineana* Pierre (Okoume) and *Pterocarpus soyauxii* Taub (Padauk), and one temperate softwood, *Abies alba* (Silver fir). A first series of 14-day tests was performed at 10% stress level and 65% relative humidity (RH), with moderate step variations at 45 and 75% RH. A second series of 5-day tests was performed at 35% stress level and 75% *RH* with a stronger step variation at 45% RH. Deflection and transverse expansion were measured using linear variable displacement transducers. The results show that the first variation of RH always increases the deflection and that subsequent changes decrease (humidification) or increase (drying) it. It was also observed that Padauk has a higher viscoelastic response and a lower mechanosorptive response than Silver fir and Okoume. As an indication of interaction between viscoelastic and mechanosorptive behaviour, in 14-day test the latter influenced the former, with small increments of relative compliance at each cycle. The analysis of the mechanosorptive trajectories suggested the existence of a creep limit and confirmed that of pseudo-creep/recovery.

List of symbols

b	Thickness due to moisture content changes (mm)
b_i	Initial thickness (mm)
E_L	Longitudinal modulus of elasticity (MPa)
E_L/ρ	Longitudinal specific modulus of elasticity (MPa)
F	Force (N)
G	Shear modulus (MPa)
h, h_i	Specimen height (mm), initial value
J	Compliance (MPa^{-1})
J^*	Effective compliance (MPa^{-1})
l	Lever arm for creep test (mm)
l_r	Lever arm for rupture test (mm)
m, m_0	Mass (g), anhydrous value
MC	Moisture content (%)
RH	Relative humidity (%)
S, S_i	Cross section (mm^2), initial value
T1,3,4,6,7,9	Lateral transducers
T2,5,8	Central transducers
V_0, V_a	Deflection (mm) at the central, lateral position
v_{Ta}, v_{TO}	Deflection due to shear force (mm) at the central, lateral position
ρ	Specific gravity
ρ_L	Specific gravity of cell wall
ε	Strain
$\varepsilon_{t\varphi}$	Corrected strain due to swelling shrinkage in transverse direction
ε_0	Instantaneous strain
ε_φ	Strain due to swelling shrinkage in transverse direction
φ	Coefficient that considers the mechanical effects on lateral transducers
θ	Temperature (°C)
σ, σ_0,	Stress (MPa), initial stress, effective stress
ω	Slope due to the rotation

✉ Rostand Moutou Pitti
rostand.moutou_pitti@uca.fr

[1] Université Clermont Auvergne, CNRS, Clermont Auvergne INP, Institut Pascal, 63000 Clermont-Ferrand, France

[2] DAGRI-Department of Agriculture, Food, Environment and Forestry, University of Florence, 50145 Florence, Italia

[3] USTM, Ecole Polytechnique de Masuku, BP 901, Franceville, Gabon

[4] Université Clermont Auvergne, INRAE, PIAF, 63000 Clermont Ferrand, France

[5] CENAREST, IRT, BP 14070, Libreville, Gabon

1 Introduction

The mechanical behaviour of wood is considerably affected by the interaction between climatic variations and mechanical load (Grossman and Kingston 1954; Pittet 1996; Randriambololona et al. 2002; Dubois et al. 2012), especially below the fibre saturation point (Llana et al. 2018). For wooden structures subject to these interactions over time, their service life is greatly reduced (Hamdi et al. 2018). Wood by its polymeric nature has the characteristics of a viscoelastic material, with a dependence on temperature and load level (Placet 2006; Bažant 1985). Several studies attempted to define the limit of linear viscoelastic behaviour; it depends on the type of test performed, the criterion on which the linearity limit is based, and the precision with which it is measured (Hunt 1989). According to Mukudai and Yata (1987), for loads less than 40% of the maximum tensile stress wood shows a linear behaviour. Randriambololona et al. (2002) placed this limit between 10 and 20% in compression and between 20 and 30% in bending or tension, Hoyle et al. (1986) for Silver fir at 40% of the bending strength and Foudjet and Bremond (1989) for tropical wood at 35%. Viscoelastic behaviour can be demonstrated by creep tests in a constant climatic environment (Navi and Heger 2005). When the effects of climatic variations under constant mechanical load are added to viscoelastic behaviour, wood exhibits another more complex behaviour called mechanosorption (Navi et al. 2002; Nguyen et al. 2016). An early work on mechanosorptive behaviour was carried out by Armstrong and Kingston (1960); they observed that the deflection of a wooden specimen was influenced by variations in relative humidity. Relaxation creep tests under mechanical stress also highlighted the effects of drying and humidification on the behaviour of wood (Ranta Maunus 1975; Engelund et al. 2012; Saifouni et al. 2016; Engonga et al. 2020; O'Ceallaigh et al. 2020; Hou et al 2021; Asyraf et al. 2021; Franke et al. 2022; Nkene Mezui et al. 2023; Aloisio et al. 2023).

From a theoretical point of view, the investigation of the time-dependent behaviour of polymers such as wood is twofold: the study of the compliance limit and the study of viscous parameters (Mohager and Toratti 1992). To date, there are several studies dealing with the viscoelastic and mechanosorptive behaviour (Peng et al. 2019; Ratanawilai and Srivabut 2022). The work of Mohager and Toratti (1992) on several mechanosorptive creep tests under different humidity cycles suggest that there is no strain limit due to mechanosorptive effects. This hypothesis had also been discussed by Gril (1988) and Montero et al. (2012) who studied the kinetics of viscoelastic creep. The results of their work have made it possible to assess a compliance limit state for very long times. A comparison of these results with the mechanosorptive effects revealed irreversible effects. The experimental approach of Hanhijärvi and Hunt (1998) and Montero et al. (2012) aimed at separating the contributions of time and moisture content variations from the viscoelastic and mechanosorptive phenomena, which however remains difficult.

Most of that work has been carried out on softwood and temperate hardwood species, or at high stress levels sometimes exceeding the viscoelastic linear limit. The use of specimens of large dimension, involving other phenomena such as moisture diffusion effect, made the study of the viscoelastic and mechanosorptive behaviour even more complex. Up to now very few studies on viscoelastic and mechanosorptive behaviour of tropical species, such as African tropical woods, have been published. Manfoumbi contributed to the application of the Eurocode 5 in the design and verification of timber constructions in tropical zones (Manfoumbi et al. 2022). He has shown, for example, that tropical woods have a delayed behaviour accentuated by the high variation in humidity for insignificant temperature variations. Houanou et al. (2014) estimated the influence of the load duration on the linear viscoelastic parameters of tropical wood in creep test. His work showed that the loading time has no influence on the dynamic modulus.

This paper presents creep data for two tropical species and one European softwood species under two different stress levels and relative humidity cycles. The time-dependent behaviour of the two tropical wood species is poorly documented. The tests were carried out at the University of Florence.

2 Material and methods

2.1 Characterization of the specimens used

Two tropical hardwoods from Gabon, *Aucoumea klaineana* Pierre or Okoume (O) and *Pterocarpus soyauxii* Taub or Padauk (P), and one softwood from Auvergne region, France, *Picea abies* or Silver fir (S), were studied. Static tests were carried out on 3 specimens per species to estimate the failure stress (Table 1). For this study, the nominal dimensions of the specimens (Fig. 1a) were 160 mm in longitudinal direction (L) for the length, 12 mm in tangential direction (T) for the thickness (height, *h*) and 6 mm in radial direction (R) for the width (*b*). For all the tests carried out on a given species, the specimens used were cut from the same block. The specimens for the 14-day test were divided into batches. For the Padauk and Okoume specimens, the first number before the dot indicates the batch number and the number after the dot indicates the specimen number. In the case of Silver fir, the batch number is indicated by a number and a letter followed by a dot which

indicates the number of the test piece. For the 5-day test, the specimens have a number that indicates the specimen number.

The specimens were initially conditioned at 65% relative humidity (RH) and a temperature (θ) of 20 °C for 7 days, then tested in 3-point bending on an AMSLER press (Fig. 1b), consisting of a static test stand with a total span (L_r) of 150 mm. The press has an automatic data (force) logging system. Once the force is obtained, the bending strength is deduced by applying the following equation, based on the assumption of a homogeneous linear relationship between stress and strain in the specimen:

$$\sigma = F \cdot Lr \cdot h/(8I) = (3/2) \cdot F \cdot Lr/(h2b) \quad (1)$$

where F is the applied load and $I = bh^3/12$ the moment of inertia. The specific gravity and failure stress of each specimen, and their mean per species, are given in Table 1.

Table 1 Characteristics and rupture stresses of the specimens tested for static fracture tests

Specimen	Species	Specific gravity (ρ)	Failure stress σr (MPa)
O8.7	Okoume	0.46	88.8
O3.5		0.51	91.7
O3.10		0.50	92.2
Mean ± standard deviation		0.49 ± 0.03	90.9 ± 1.8
P4.11	Padauk	0.77	126.3
P4.17		0.77	141.3
P4.20		0.76	102.2
Mean ± standard deviation		0.77 ± 0.01	123.3 ± 19.7
S4C.2	Silver fir	0.41	75.1
S4C.5		0.45	81.6
S4C.9		0.40	71.9
Mean ± standard deviation		0.42 ± 0.03	76.2 ± 5.0

2.2 Creep tests

The creep tests were started after the rupture tests. Figure 2a shows the entire experimental set-up for the first three trials, conducted over 14 days and carried out in pairs (Fig. 2b): test $T^{14}{}_1$ on Okoume and Silver fir, test $T^{14}{}_2$ on Padauk and Okoume and test $T^{14}{}_3$ on Padauk and Silver fir. Figure 2c shows the plastic support for fixing the load on the specimen during loading, made with a 3D printer. For these tests the specimens were loaded at 65% RH, subjected to two humidification cycles at 75% RH and one drying cycle at 45% *RH,* then unloaded at 65% RH and subjected to a humidification cycle at 75% RH.

For the second series of tests, conducted over 5 days, the device was improved by adding a third bench (Fig. 2d) and by putting the loading system outside the box for high loads. These adjustments allowed us to test all three species simultaneously and did not alter the overall functioning of the experimental set-up. The whole device was now composed of 3-point bending creep test benches. The results of 3 tests ($T^5{}_1$, $T^5{}_2$, $T^5{}_3$) will be presented. In this series of tests, the reference humidity was 75% RH, with one drying cycle down to 45% RH during the loading phase and no humidity change after unloading. Figure 3 shows a schematic drawing of a test bench equipped with transducers: the total length is 160 mm and the lever arm ($L/2$) 70 mm. The distance between the transducers is 60 mm so that the gap between the position of each lateral transducer and the corresponding loading support is 10 mm. The study of creep at 65% and 75% RH was carried out to observe the viscoelastic behaviour of wood in an initial dry state (65% RH) and in an initial wet state (75% RH).

In both series of tests, each bench was composed of 3 transducers, two at the ends and one in the centre. The lateral transducers (T1, T3, T4, T6, T7, T9) allow estimating the transverse expansion along the height of the specimen and correcting the central deflection measured by the transducers at the centre (T2, T5, T8), as will be explained below;

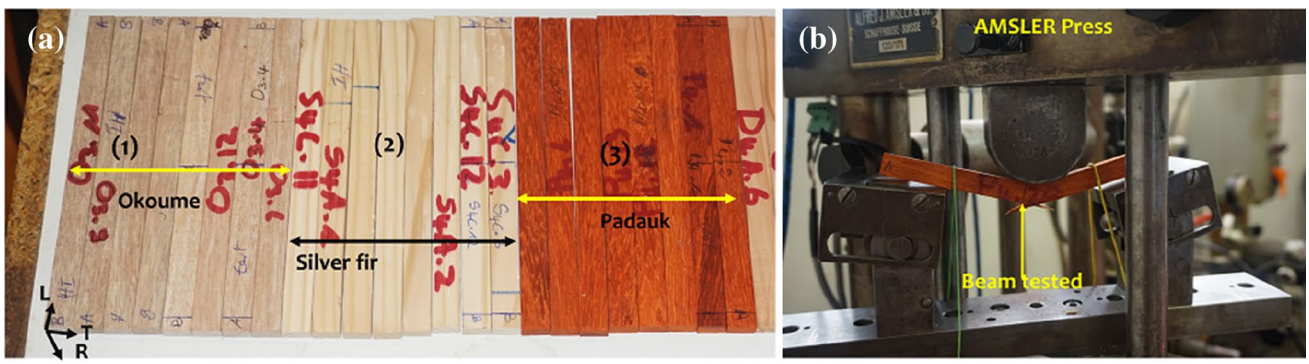

Fig. 1 Experimental setup for rupture test: **a** specimens of Okoume (1), Silver fir (2) and Padauk (3); **b** AMSLER press test bench

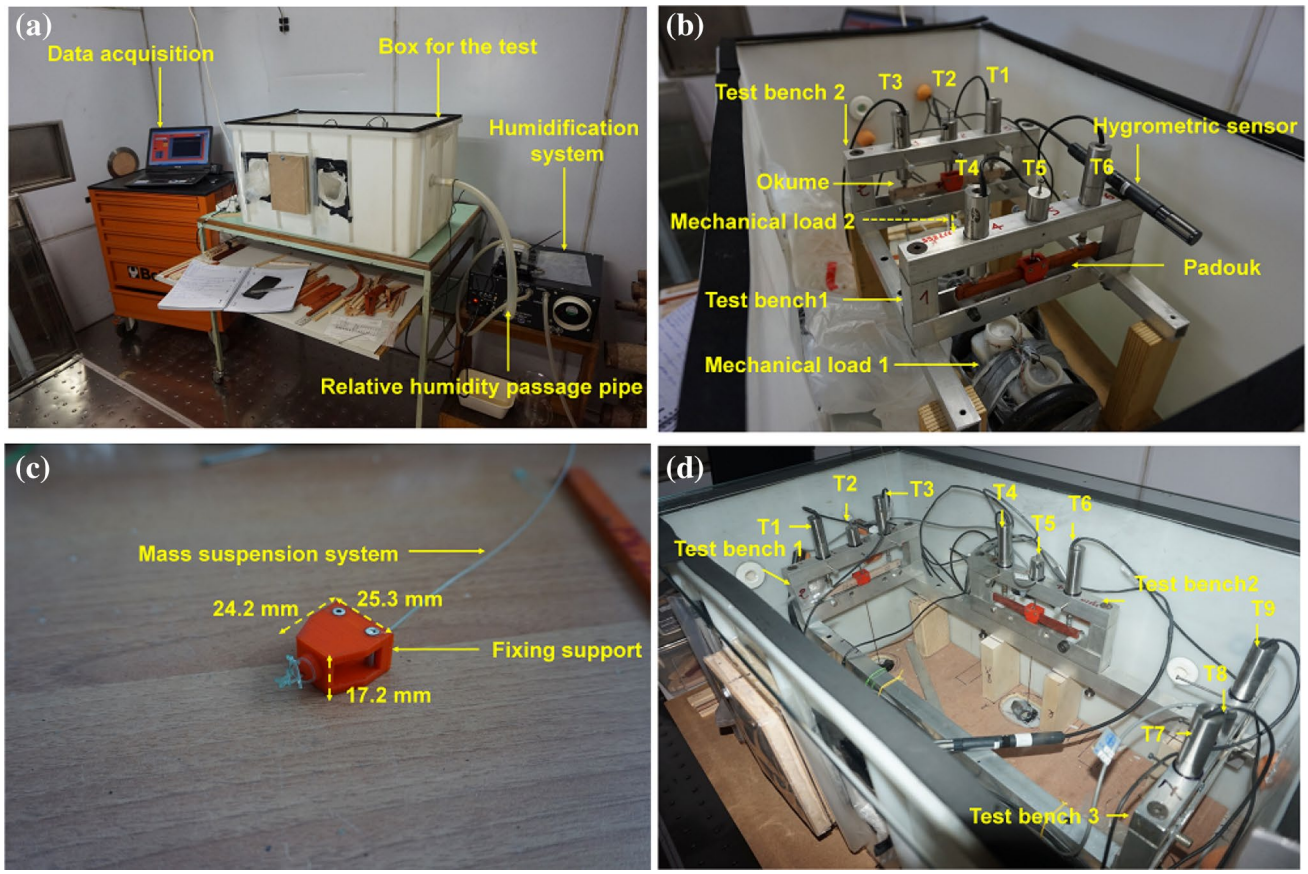

Fig. 2 Experimental setup: **a** overall experimental set–up; **b** view of the two creep benches for the 14-day creep test; **c** plastic support for the application of the load; **d** view of the three creep benches for the 5-day creep test

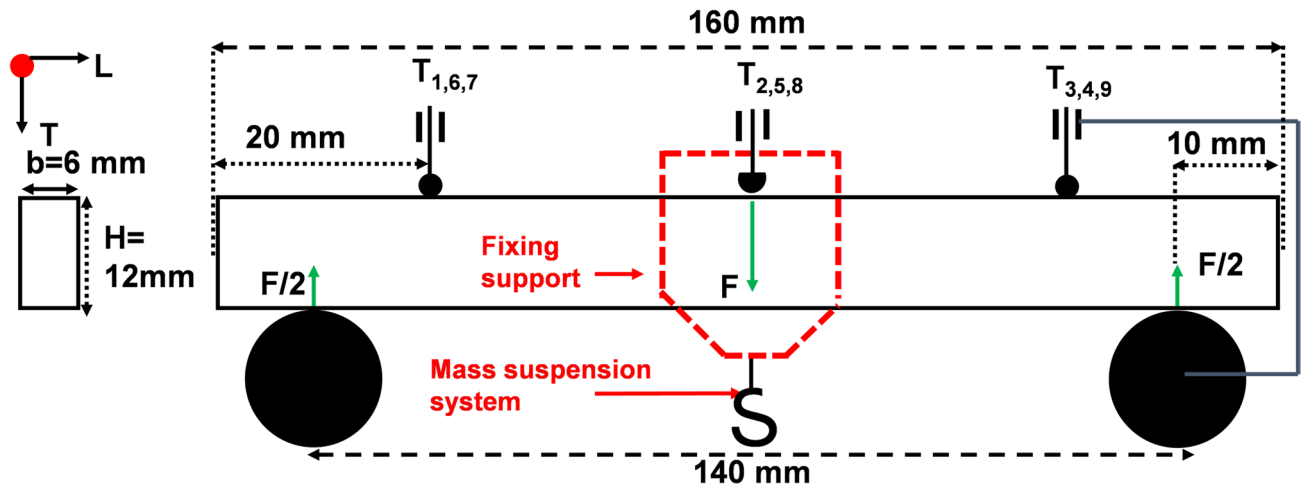

Fig. 3 Schematic view of a test bench equipped with transducers T

transducers T7 to T9 were only used in the second series. Figure 3 illustrates the placement of the transducers. The benches were placed in a box hermetically sealed with a transparent window, of dimensions (750 × 450 × 450 mm) and equipped with two thermo-hydro sensors for monitoring θ and RH, controlled by means of a pump diffusing the humidity in the box through a pipe. The humidification system used was precisely regulated and was a scale model of

Preservatech's type MINI ONE positive pressure humidity controller. The experimental set-up (the box) was exposed in a large climatic room where the temperature was maintained at 20 °C and the RH at 65% for the tests. A preliminary study was carried out to determine the capacity of the controller (Preservatech MINI ONE) to keep a constant RH inside the box. For a set-point of 75% the controller has shown a cyclic sinusoidal behaviour varying between a minimum of 74.7% and a maximum of 75.3% of relative humidity (±0.3% RH), confirming the optimal performance of the environmental control. For all tests carried out, control specimens of the same size were also placed in the box to estimate the moisture content (*MC*) by mass monitoring, using 4 specimens per species in the first series, 5 per species in the second. The specimens were taken out of the box to be weighed, via holes made in the sides of the box. This operation did not disturb the water status of the box. When they were taken out, they were placed in an isothermal bag to limit contact with the external environment before being weighed. Once weighed, the samples were returned to the box via the holes. Their mass m was measured in this way occasionally, before and during the creep experiments, and their *MC* calculated as:

$$Mc - Exp(\%) = (m - m_0)/m_0 \quad (2)$$

where m_0 is the anhydrous mass and *Mc-Exp* stands for experimental *MC*. Table 2 shows the specific gravity (ρ) and initial *MC* of each control specimen before each series of tests.

Note that the placement of the cross-section, placed vertically along the T direction characterised by a slower diffusion, has been designed to favour the horizontal gradients of moisture content in the transient phases during the humidity steps. At the same time, it reduces the sensitivity to the tangential surface cutting through earlywood or latewood, the upper and lower faces that most contribute to bending being radial sections.

Table 3 gives, for each specimen tested in creep, the test number, specific gravity and stress level applied, calculated as the ratio between the applied stress σ and the mean failure stress per species σ_r given in Table 1.

Table 3 Characteristics of specimens and stress level for the 14-day and 5-day test

Specimen	Species	Test number	Specific gravity (ρ)	Stress level (σ/σ_r)
O3.2	Okoume	T^{14}_1	0.49	10%
O3.1		T^{14}_2	0.48	10%
O2		T^{5}_1	0.41	35%
O5		T^{5}_2	0.41	35%
O1		T^{5}_3	0.41	35%
P4.1	Padauk	T^{14}_2	0.78	10%
P4.23		T^{14}_3	0.75	10%
P1		T^{5}_1	0.76	35%
P3		T^{5}_2	0.76	35%
P6		T^{5}_3	0.78	35%
S4C.4	Silver fir	T^{14}_1	0.42	10%
S4C.12		T^{14}_3	0.4	10%
S2		T^{5}_1	0.41	35%
S10		T^{5}_2	0.45	35%
S12		T^{5}_3	0.4	35%

Table 2 Properties of the control specimens for the 14-day and the 5-day test

14-day test				5-day test			
Specimen	Species	Specific gravity (*ρ*)	Initial *MC* (%)	Specimen	Species	Specific gravity (ρ)	Initial *MC* (%)
O3.3	Okoume	0.49	11.2	O9	Okoume	0.40	13.35
O3.9		0.48	11.69	O11		0.41	13.44
O3.8		0.47	11.18	O16		0.44	13.25
O3.11		0.49	11.32	O17		0.41	13.43
				O33		0.40	13.27
S4A.2	Silver fir	0.40	11.11	W2	Silver fir	0.41	13.62
S4A.3		0.40	11.06	W4		0.42	12.86
S4A.1		0.42	10.94	W8		0.44	13.35
S4A.4		0.42	11.54	W15		0.38	13.44
				W17		0.39	12.66
P4.8	Padauk	0.81	8.67	P8	Padauk	0.73	10.96
P4.14		0.76	8.53	P13		0.71	10.62
P4.16		0.77	8.25	P15		0.70	11.10
P4.19		0.80	8.55	P23		0.70	10.80
				P24		0.70	10.90

2.3 Analysis of the creep tests at changing moisture content

The analysis is based on the application of Bernoulli–Euler beam theory, assuming linear relationship between stress and strain and homogenous properties and moisture content within the specimen. For a small perturbation the strain ε as a function of space and time t can be expressed as:

$$\varepsilon(x,y,t) = \varepsilon_0(t)(1-2x/L)(1-2y/h) \tag{3}$$

where L is the total span ($L=140$ mm) and ε_0 the maximum tensile strain in the centre of the beam, and the deflection v(x, t) verifies:

$$\partial^2 v/\partial x^2 = \partial\varepsilon/\partial y = (2\varepsilon_0/h)(1-2x/L) \tag{4}$$

The time-dependent compliance $J=\varepsilon/\sigma$ being assumed independent of the position, the stress distribution is (Fig. 4a):

$$\sigma(x,y,t) = J(t)\varepsilon(x,y,t) = \sigma_0(t)(1-2x/L)(1-2y/h) \tag{5}$$

where σ_0 is the maximum tensile stress, given like in Eq. (1) by:

$$\sigma_0 = (1/J)\varepsilon_0 = L.F.h/(8I) = (3/2).L.F/(h^2 b) \tag{6}$$

By successive integration of Eq. (4) we get the expression of the slope ω and the deflection v, as:

$$\omega = \partial v/\partial x = (\varepsilon_0 L/2h)\omega_1(2\xi-\xi^2); \quad v = v_0(1-3\xi^2/2-\xi^3/2) \tag{7}$$

where $\xi=2x/L$ is the relative axial position, and ω_1 the maximum slope (for $\xi=1$) and v_0 the maximum deflection (for $\xi=0$) are given by:

$$\omega_1 = \varepsilon_0 L/(2h); \quad v_0 = -\varepsilon_0 L^2/(6h) \tag{8}$$

The central transducer being placed at position $x=0$ above the specimen while the support points B are placed below (Fig. 4b), its measurement includes the height variation h and the deflection due to the trenching force v_{T0}:

$$V_0 = -v_0 - \Delta h - v_{T0} = \varepsilon_0 L^2/(6h) - \Delta h - v_{T0} \tag{9}$$

with $v_{T0}=(6/5)\cdot(h/L)^2\,(E/G).v_0$; E is the modulus of elasticity and G is the shear modulus. In our case the ratio (E/G) is 12.9 for Padauk, 16.6 for Silver fir and 13.6 for Okoume: these values were obtained thanks to dynamic tests carried out using 'Bing' method, based on the measurement of the first resonance frequencies of free-free vibration in bending mode (Brancheriau and Paradis 2007). The lateral transducers are also placed above the specimen at position A, at a small distance $\alpha\cdot L/2$ ($\alpha\sim 1/7$) from the corresponding support point B. The measured displacement is given by:

$$V_a = -v_a - \Delta h a - v_{Ta} = -\phi v 0 - \Delta h - v_{Ta}; \varphi = (3\alpha/2)(1-\alpha^2/3) \tag{10}$$

where v_a is the deflection at position $\xi=1$-α and Δh_a is negligibly influenced by the slope at this position and $v_{Ta}=(6\alpha/5)\cdot((h/L)^2\cdot(E/G)\,v_0$.

The effect of such rotation of the neutral axis on V_0 and V_a is negligible as well, thanks to the small value of ω. Coefficient φ considers the mechanical effects on lateral transducers, its theoretical value is given in Eq. (10). However, this parameter will be determined experimentally by calculating the slope between v_a and v_0 during loading and unloading. The slope between V_a and V_0 is defined as follows:

$$V_a = \varphi \cdot V_0 \tag{11}$$

In practice, it turned out that this value of φ was not the same during loading and unloading. This difference can be explained by several factors such as the contact effects of the beams on the supports, and by a small difference of moisture content.

The variables ε_0 and Δh can be derived from the expressions of V_0 and V_a given by Eq. (9) and Eq. (10):

$$\varepsilon_0 = (6h/L^2)\cdot(V_0 - V_a)/(1-\varphi+\lambda) \tag{12}$$

$$\Delta h = ((1+\lambda)V_a - (\varphi+\lambda\alpha)V_0)/(1+\lambda-(\varphi+\alpha)) \tag{13}$$

where $\lambda=(6/5)\cdot((h/L)^2\cdot(E/G)$. The compliance $J(t)$ could be obtained as the ratio ε_0/σ_0 from Eq. (6) and Eq. (12). However, in a creep test, the load F is kept constant, not the stress. When the moisture content changes, so do the transverse dimensions h and b, and consequently the stress:

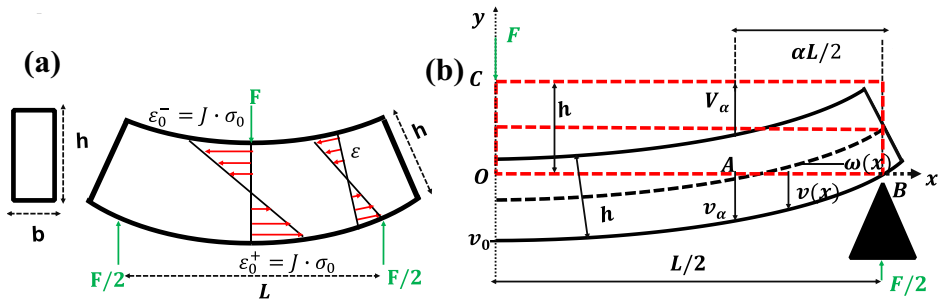

Fig. 4 Application of beam theory: **a** stress and strain distribution in the specimen; **b** deflection and measured displacement

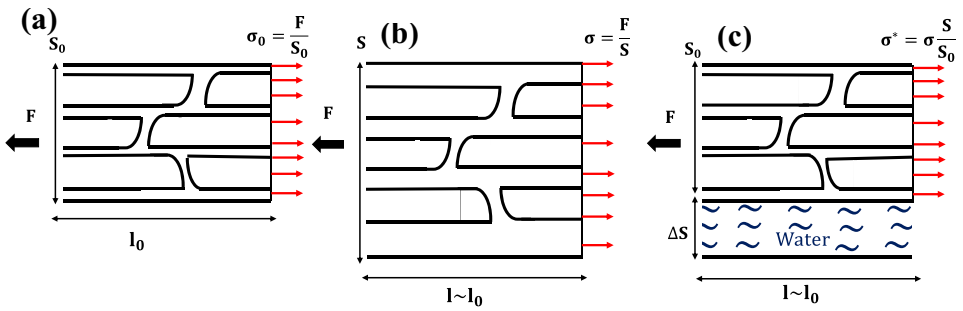

Fig. 5 The effective (nominal) stress in the longitudinal direction of wood: **a** initial dry state; **b** swollen wet state; **c** equivalent to the wet state in fibre direction

the test is no longer, strictly speaking, a creep test. But in the case of a test performed in the fibre direction of wood, the variation of cross section is mostly due to the deposition of water layers in the cell wall, that do not support a significant part of the load (Fig. 5); it is appropriate for the creep analysis to consider as effective the nominal stress σ^*, ratio of axial load to initial cross section, related to σ by:

$$\sigma^* = (S/S_i)\sigma \tag{14}$$

where $S = bh$ is the cross section and $S_i = b_i h_i$ its initial value. In a tensile creep test, σ^* thus defined would remain constant. In bending creep, variations of σ^* exist although attenuated compared to those of σ:

$$\sigma^* = (hb/h_i b_i)\sigma = [(3/2)L \cdot F/(h_i{}^2 b_i)]/(1+\varepsilon_t) \tag{15}$$

where $\varepsilon_t = \Delta h/h_i$ is the relative variation of specimen height, or transverse expansion since the time of loading. Since the moisture-induced variations of wood in the L direction remain small, such a correction is not needed for the strain ε. Consequently, for small fluctuations of σ^*, according to Eq. (12) and Eq. (15) the effective compliance J^* becomes:

$$J*(t) = \varepsilon_0/\sigma_0 = [(4h_I{}^3 b_i)(1-\varphi+\Omega)/(L^3 F)][V_0(t) - V_a(t)][1+\varepsilon_t] \tag{16}$$

where σ_0 has been calculated from Eq. (6). By replacing the stress by the nominal stress, and the compliance by a nominal compliance, we eliminate the geometrical effect of cross-section variation, and retain only the behavioural contribution to the softening effect of water. Such corrections are useful for the purpose of understanding and separating effects, whereas for practical applications it is preferable to avoid them.

3 Results and discussion

3.1 Transverse expansion and estimation of moisture content

Figure 6a and b show the average evolution of shrinkage measured by the two lateral transducers (V_a) for Okoume and Padauk. In addition to shrinkage, the transducers also measure the effects of mechanical loading (φ) as can be seen at the beginning and end of loading.

In Fig. 6c and d the transverse expansion ($\varepsilon_t = \Delta h/h_i$) is obtained by elimination of the mechanical contribution using Eq. (13) and the estimate of parameter φ as defined by Eq. (11). However, a discontinuity remains at unloading. Thanks to an adjustment of φ value at unloading, continuous curves are obtained as in Fig. 6e and f, where the transverse strain ε_t has been obtained by eliminating the mechanical contribution during loading and unloading. We determined the moisture content of the specimens by linear correlation between the water deformations (ε_t) and the experimental measurements of the moisture content *(Mc-Exp)* given by Eq. (2):

$$Mc(t) = \gamma \varepsilon_t(t) + \kappa \tag{17}$$

where the constants (γ, κ) are fitted from cycle to cycle to have a better coefficient of determination.

Figures 7 and 8 show the evolution of *MC* for the specimens of 14-day and 5-day test, respectively. On all curves we can see a good correlation between the experimental points (*Mc-Exp*) and the points obtained by correlation (*Mc-Int*). However, an isolated *MC* value can be observed in Fig. 7c for Padauk; this can be explained by an erroneous measurement of the mass when taking the measurements. The lack of experimental points between the end of the first day and the 4th day of the test is due to the laboratory being closed on weekends so that we could not measure the mass of the specimens. However, the analysis gave us an idea of the moisture content of the specimens tested during these periods.

3.2 Creep and recovery tests

Figures 9 and 10 show the results of creep and recovery tests at 35% and 10% stress level for the 14-day and 5-day test, respectively. The maximum strain ε_0 has been calculated according to Eq. (11). After loading the specimens, instantaneous strain is observed (a_0-a_1) followed by viscoelastic strain at constant humidity (a_1-a_2) then creep at varying humidity (a_2-a_3). Unloading provokes an instantaneous recovery (a_3-a_4) followed by a delayed recovery (a_4-a_5). In the 3rd 14-day test (Fig. 9c) the end of Padauk data is

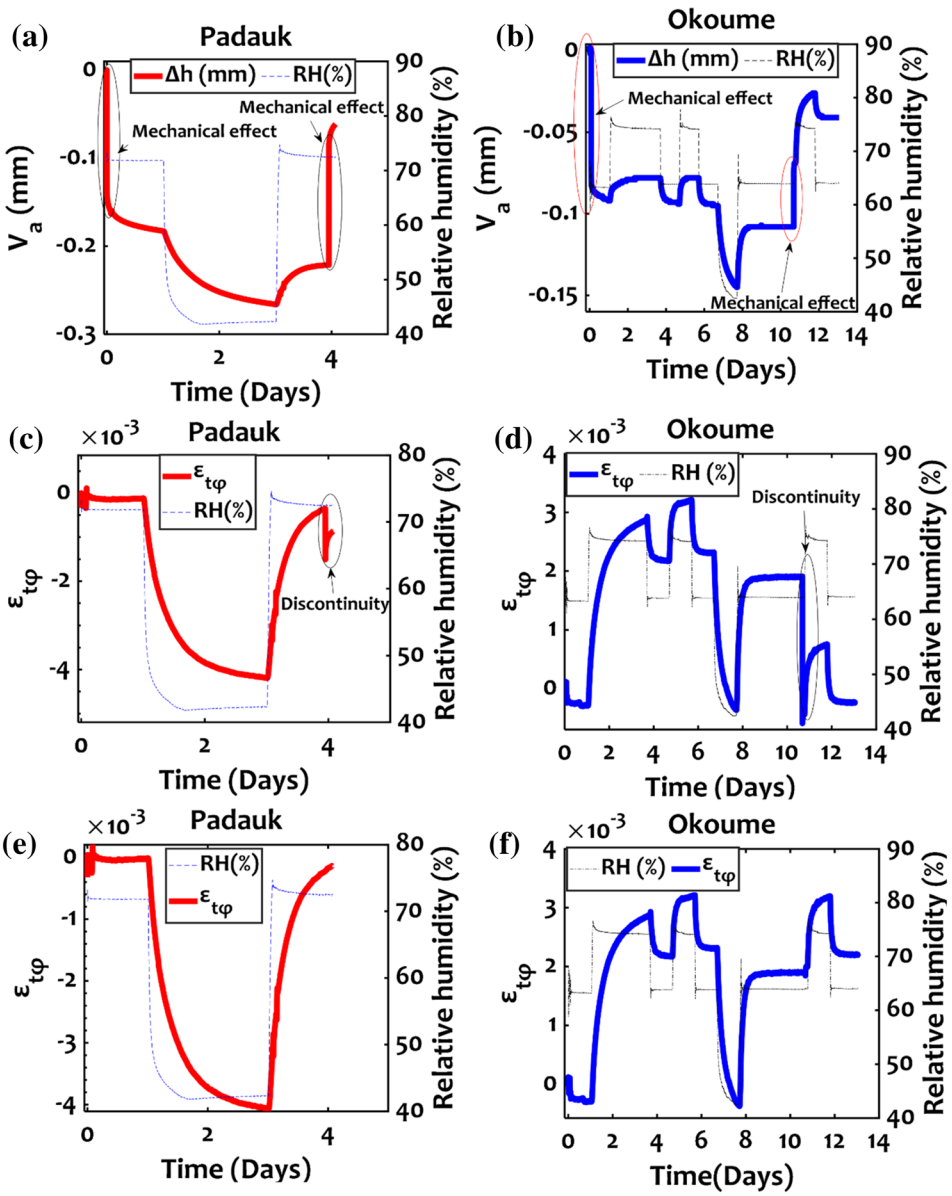

Fig. 6 Transverse expansion; **a**, **b** swelling shrinkage of 5-day test and 14-day test; **c**, **d** strain due to the swelling shrinkage of species; **e**, **f** strain corrected for the mechanical effects

missing because of a problem with the sensors on the 11th day. Although the same stress level has been applied to all specimens, both their instantaneous and delayed response differ markedly. The observed strain is generally greater in Padauk and lower in Silver fir; in the first series the two tested specimens of Okoume exhibited extremely contrasted responses, while it was intermediate for the three specimens in the second. Step humidity variations under load always result in strain increase in the case of first wetting (Fig. 9) and drying (Figs. 9 and 10); for subsequent wetting, either a recovery or a small increase is observed. Such features are typical of the mechanosorptive behaviour of wood subjected to bending creep (Ranta-Maunus 1975) and will be analysed in more detail below. According to Hunt (2004), although both humidification and drying under load contribute equally to the mechanosorptive creep, an additional and reversible effect leads to an apparent difference, pseudo creep during drying and pseudo recovery during wetting. This phenomenon has been interpreted by Hunt as a difference of longitudinal hygroscopic expansion of the wood subjected to tension and compression. As a result, drying steps induce more creep than wetting steps, with sometimes apparent recovery observed during wetting steps, with the exception of the first wetting where the contribution of viscoelastic creep, triggered by the higher humidity, dominates the mechanosorptive response—thus explaining the so-called + + effect. In any case, the net result of the humidity variations under load (a_2-a_3) is a significant strain increase, that can be mostly attributed to mechanosorptive creep, with an unknown contribution of viscoelastic creep. At the beginning of the first

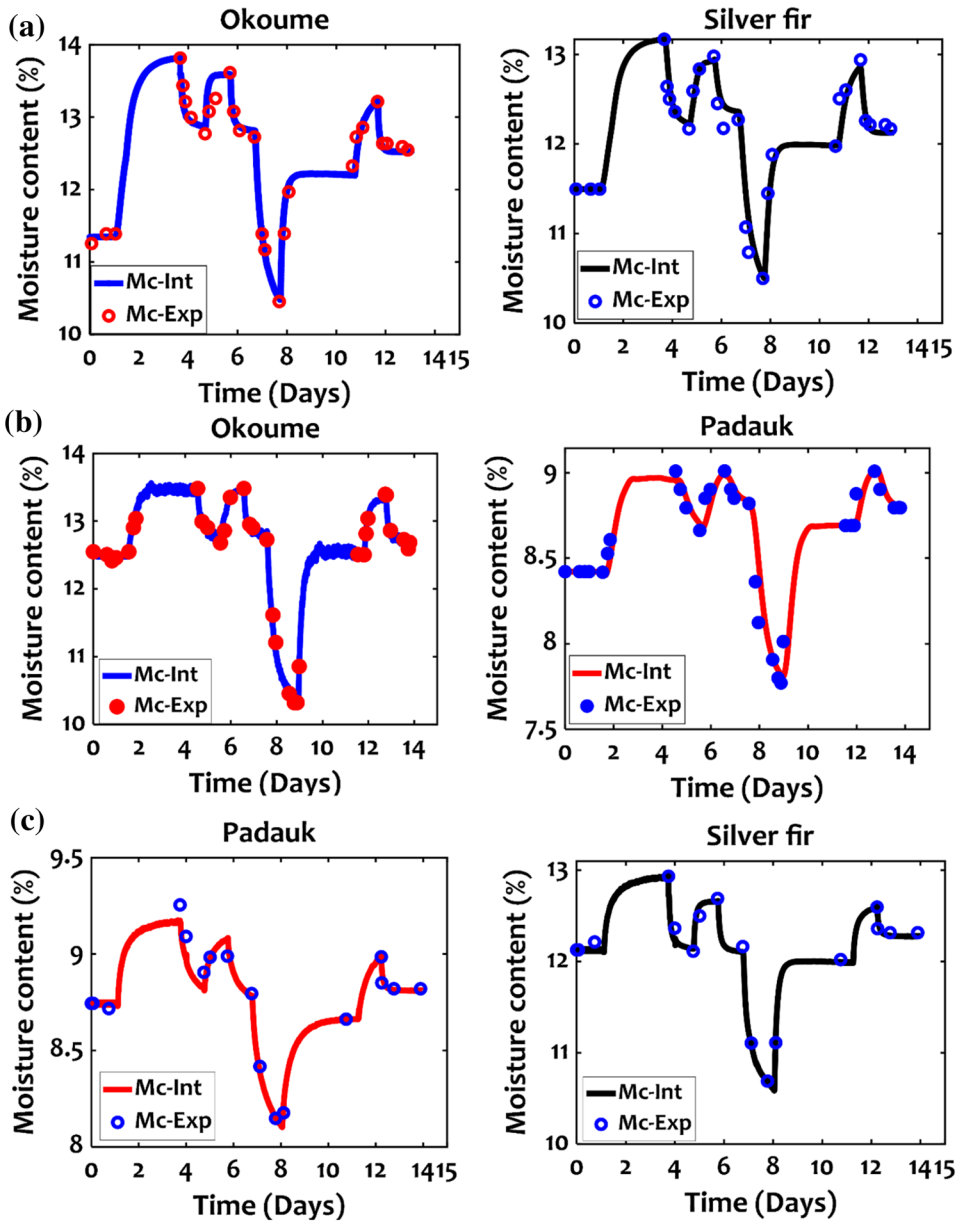

Fig. 7 Evolution of MC of control specimens for the three 15-day tests; **a** test 1, Okoume and Silver fir; **b** test 2, Okoume and Padauk; **c** test 3, Padauk and Silver fir. Open circles: occasional measurements on matched specimens (*Mc-Exp*); continuous lines: result of the interpolation (*Mc-Int*)

humidification (Fig. 9b), before the second day, the strain tended to decrease slightly as shown by the circled areas (ph). The observed behaviour is due to moisture expansion phenomena: after humidification at 75% RH, a slight peak in RH is observed, followed by a rapid decrease in RH leading to transitory shrinkage. The same observations were also made by Hunt (1994).

In the 14-day test, for Okoume and Silver fir the humidification after unloading triggered the recovery, while in Padauk it had no visible effect, which could be explained by the slower diffusion. For all the tests carried out, we note that the specimens present a memory effect because the instantaneous deformation is equal or slightly lower than the instantaneous recovery (Navi et al. 2002). The tests carried out on Padauk and Okoume do not show the memory; this can be explained by a malfunction of the sensor due to the frictional effects of the sensor during discharge. So, on the Silver fir this memory effect can be observed. From the tests carried out we notice that Padauk has a higher instantaneous deformation than Okoume and Silver fir. To better analyse this effect, we will determine the elastic parameters of these species in the following section. Figure 11 shows in concrete terms the phenomenon of pseudo-creep and pseudo-recovery. The pseudo-creep is characterized by an increase in deflection during drying and the pseudo-recovery by a decrease in deflection during wetting, due to expansion influenced by deformation.

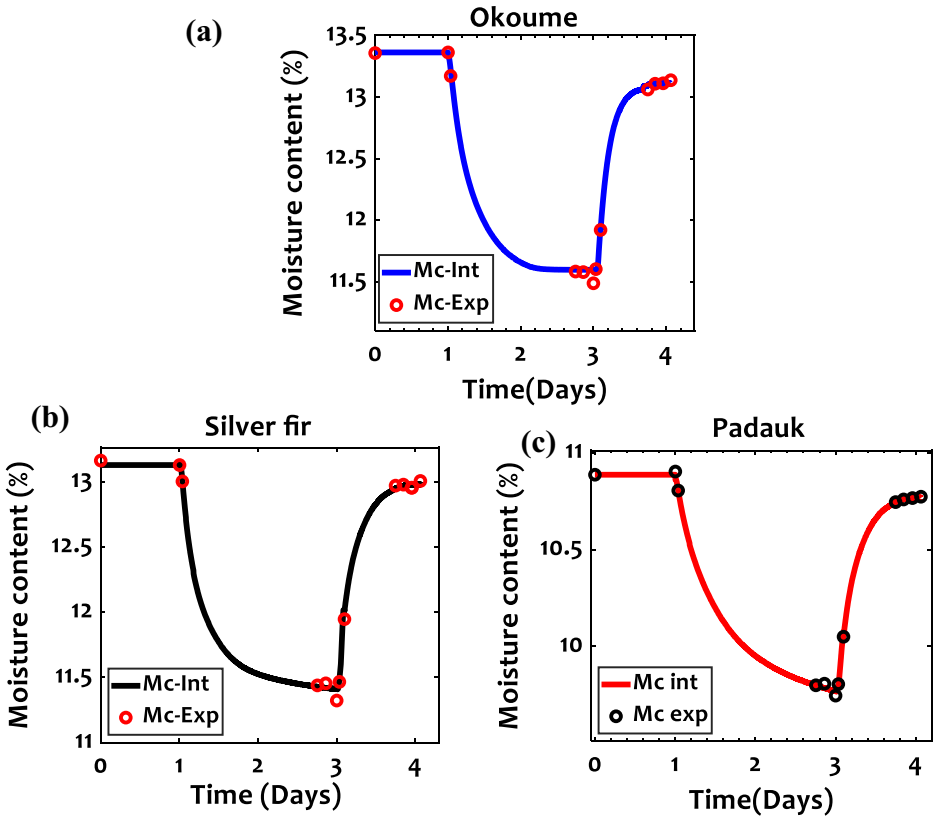

Fig. 8 Evolution of moisture content by linear interpolation of control specimens for the 5 days test; **a** Okoume; **b** Silver fir; **c** Padauk. Open circles: occasional measurements on matched specimens (*Mc-Exp*); continuous lines: result of the interpolation (*Mc-Int*)

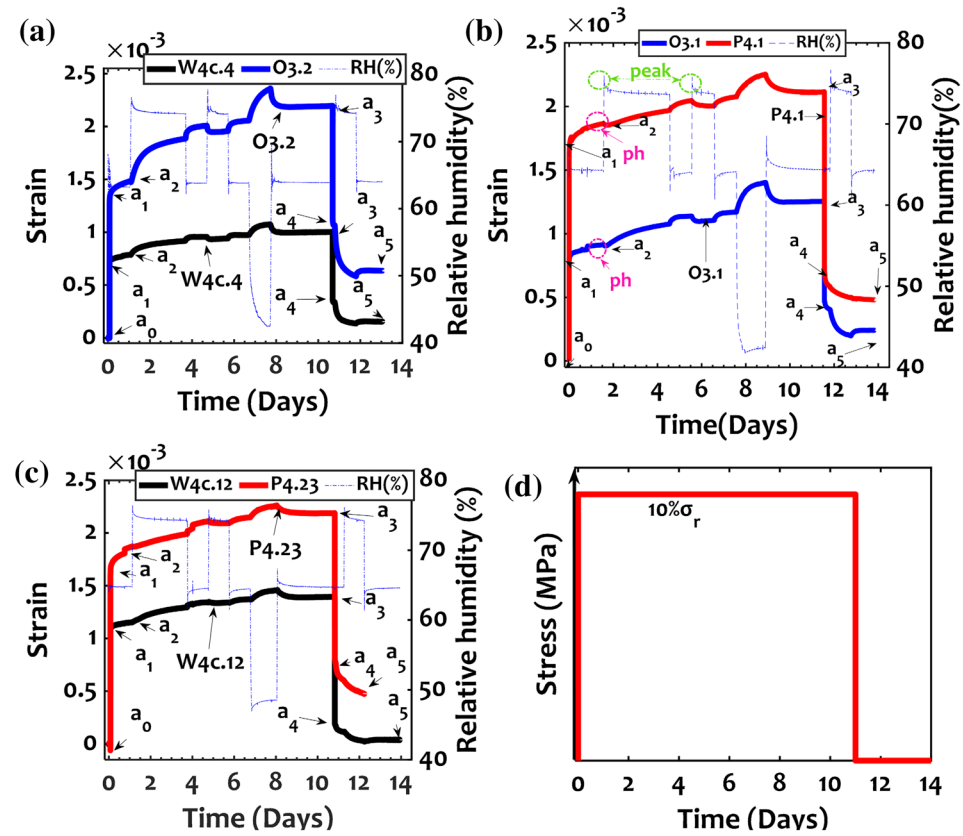

Fig. 9 Creep at 10% stress level for 11 days followed by recovery for 3 days: **a** test 1, Okoume (O3.2) and Silver fir (S4C.4); **b** test 2, Okoume (O3.1) and Padauk (P4.1); **c** test 3, Padauk (P4.23) and Silver fir (S4C.12); **d** Stress history

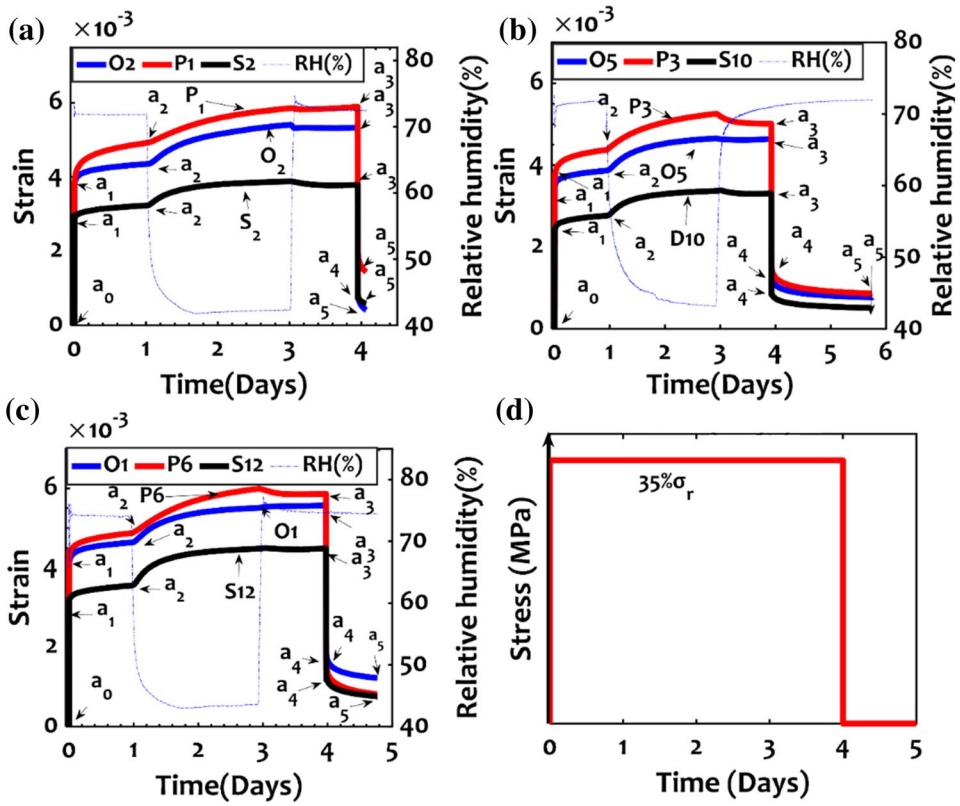

Fig. 10 Creep at 35% stress level for 4 days followed by 0–2 days of revovery; **a** test 1, Okoume (O2), Padauk (P1) and Silver fir (S2); **b** test 2, Okoume (O5), Padauk (P3) and Silver fir (S10); **c** test 3, Okoume (O1), Padauk (P6) and Silver fir (S12); **d** applied stress

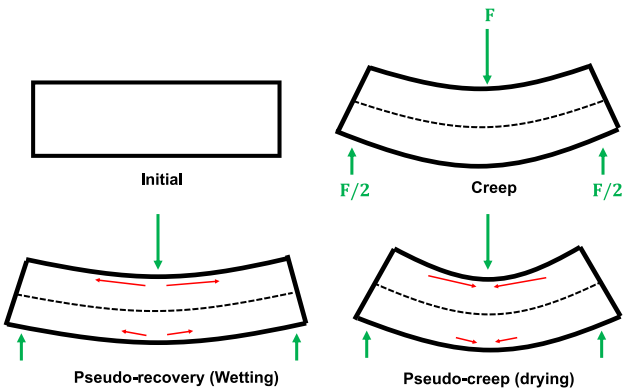

Fig. 11 Explanation of pseudo creep/recovery: deflection decrease during wetting and increase during drying, due to expansion influenced by the deformation

3.3 Analysis of the elastic response

The calculation of the elastic moduli requires the measurement of the instantaneous strain. First, the initial time t_0 is estimated by considering the average time between a_0 and a_1 (Fig. 12a). Then, the strain $\varepsilon_0(t)$ calculated according to Eq. (11) is plotted against the logarithm of time, expressed in second (Fig. 12b) so that the beginning of the viscoelastic response can be fitted to a straight line; the y-intercept is the elastic strain ε_1, defined at time $t_1 = t_0 + 1$ s, one second from the beginning of the test. Note that ε_1 is not actually an actually measured strain, but an extrapolation to a lower time range. The longitudinal Young's modulus (E_L) of the specimen can be calculated as:

$$E_L = 1/J(t_1) = \sigma_0/\varepsilon_1 \tag{18}$$

using the expression of stress σ_0 given by Eq. (6). Table 4 gives for each specimen the value of ε_1 and E_L. The specific modulus E_L/ρ is also given in the Table, as an indicator of the well-wall rigidity and mean microfibrillar angle.

The instantaneous deformations of Padauk and Okoume are close. E_L values found are slightly lower than literature values for Padauk and Silver fir (Cerre et al. 2017). For Okoume, an unusually high rigidity has been obtained especially with specimen 03.1. Overall, it appears that Silver fir and Okoume have a much greater specific modulus than Padauk, indicating a smaller mean microfibril angle in the S2 layer (MFA).

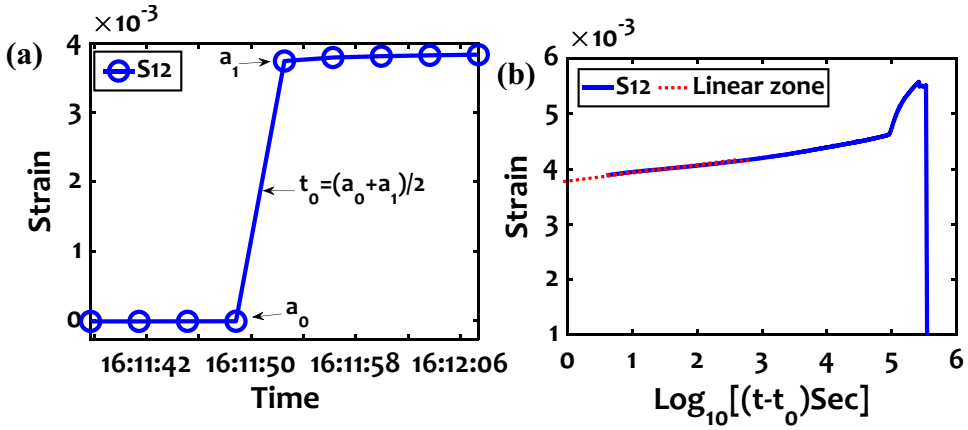

Fig. 12 Estimation of the instantaneous parameters; **a** estimation of the initial time (t_0); **b** estimation of the instantaneous strain and the Young's modulus (*MOE*)

Table 4 Elastic properties

Okoume				Padauk				Silver fir			
nb	ε_1	E_L (GPa)	E_L/ρ (GPa)	nb	ε_1	E_L (GPa)	E_L/ρ (GPa)	nb	ε_1	E_L (GPa)	E_L/ρ (GPa)
O3.2	0.11	8.0	16.4	P4.1	0.12	11.2	14.3	S4.C4	0.06	11.1	26.4
O3.1	0.06	14.3	29.8	P4.23	0.15	9.2	12.2	S4C.12	0.08	9.1	22.8
O2	0.30	10.7	26.1	P1	0.29	14.4	18.9	S2	0.24	11.1	27.1
O5	0.31	10.5	25.5	P3	0.31	13.3	17.6	S10	0.19	13.7	30.4
O1	0.37	8.9	21.7	P6	0.37	11.2	14.4	S12	0.26	10.1	25.3
Mean		10.5	23.9			11.8	15.5			11.0	26.4
s.d		2.4	5.1			2.0	2.7			1.7	2.8

ε_1: elastic strain (at 1 s); s.d. standard deviation

3.4 Mechanosorptive trajectories

Based on the observation that mechanosorptive effect is time-independent (Grossman 1971), Hunt (1986) proposed the use of mechanosorptive trajectories giving the compliance as a function of *MC*. They have been constructed here for Okoume, Silver fir and Padauk using Eq. (16) for the corrected compliance J^* and Eq. (17) for the *MC*. Figure 13 shows the mechanosorptive trajectories of the 5-day test, where the initial loading of the specimens was done at 75% RH and only one drying cycle was applied. Silver fir differs from Okoume and Padauk in having a slightly lower instantaneous compliance (C_0-C_1). The first variation in humidity (in drying C_1-C_2) led to a compliance increase known as the (−) effect. As already visible in Fig. 10, subsequent moisture changes, known as the (+) effect, are either marked by a slight decrease or increase in compliance.

Figure 14 shows the mechanosorptive trajectories of the 14-day test; on these figures for a better visualization the instantaneous compliance is not fully represented. The loads were applied in a dryer state (65% *RH*). The tests show the effects of the moisture content on the compliance. We note that the instant compliance of Padauk is high compared to Okoume and Silver fir. It appears after the instantaneous loading (C_0-C_1) that the first adsorption (C_1-C_2) led to a drastic compliance increase indicated here as (++) effect (Ranta-Maunus 1975; Hanhijärvi and Hunt 1998; Gril 2015). After the first adsorption phase, the subsequent changes in moisture content (C_2-C_3, C_3-C_4) did not lead to a significant increase in compliance. On the other hand, the last phase of sorption (C_4-C_5, C_5-C_6), marked by a significant drying, did lead to a compliance increase. These results are strongly marked by the phenomenon of pseudo-creep and pseudo-recovery during the successive drying and wetting phases. Above all, it appears that the mechanosorptive effect is not very important or pronounced after the first humidification phase. The slope of the observed trajectories is similar to that of the evolution curves of the compliance of Hunt (1989) and seems to highlight the

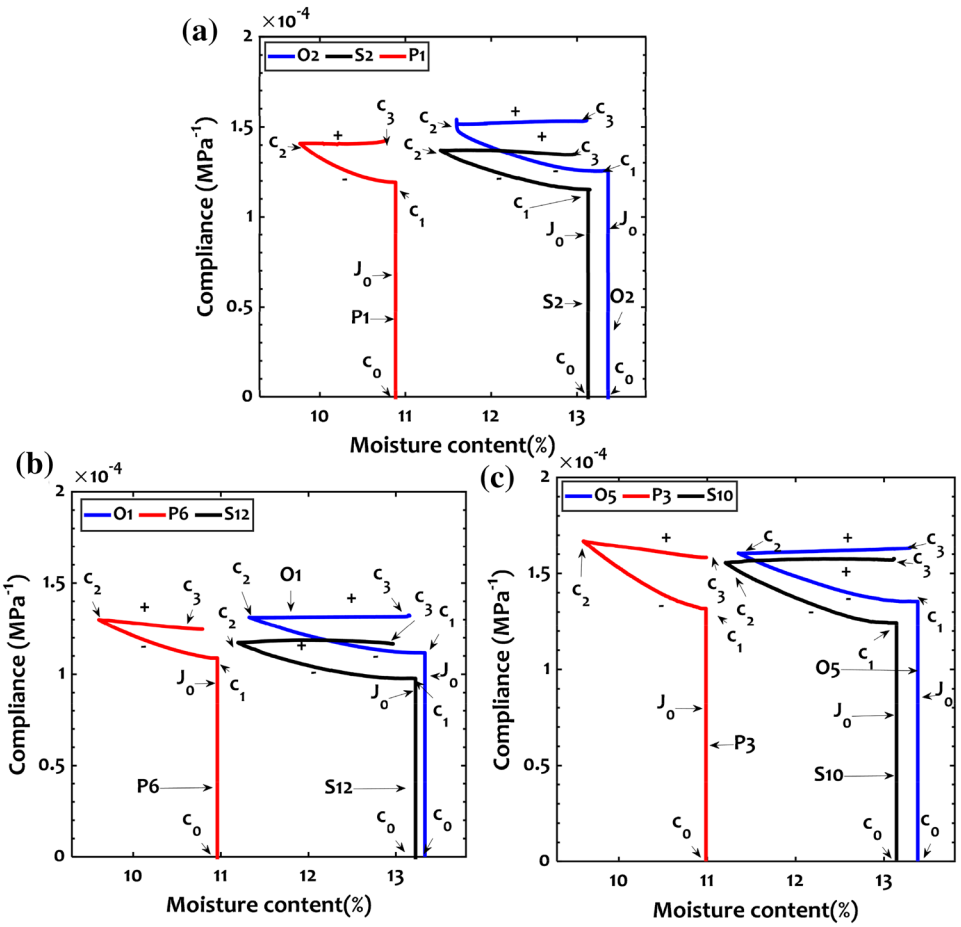

Fig. 13 Mechanosorptive trajectories (J*) of 5 days; **a** test 1 Okoume (O2), Silver fir (S2) and Padauk (P1); **b** test 3 Okoume (O1), Silver fir (S12) and Padauk (P6); **c** test 2 Okoume (O5), Silver fir (S10) and Padauk (P3) (C_0, C_2 and C_3 = sorption cycle); J_0 instantaneous compliance

existence of a marked limit creep for our tests. Indeed, we notice that the straight lines tend to be superimposed at each sorption cycle.

3.5 Interaction between viscoelasticity and mechano-sorption

In this section we will attempt to separate the contribution of viscoelasticity and mechanosorption to the time-dependent behaviour. First, let define the relative creep of a specimen as:

$$X(t) = J*(t)/J_0 - 1 \tag{19}$$

where $J_0 = 1/E_L$ is the elastic compliance estimated at 1 s, according to Eq. (18). Figure 15 shows, in the case of Okoume, the relative creep of all tests performed in a logarithmic time scale. In the first part of the curves, corresponding to the creep at constant humidity observed during the first day, a linear fit was applied during the period defined by $-0.5 < log_{10}(t) < 0$ (t in days) and used to extrapolate the viscoelastic behaviour over 14 or 5 days, depending on the test. At $tf = 11$ days or 4 days, respectively (just before unloading), the humidity has returned to that of the first day of the test. The extrapolated value X_{VE} at tf is taken as the final value of the relative viscoelastic creep, and the difference X_{MS} with $X(t_f)$ as the final value of the relative viscoelastic creep:

$$X_{MS} = X(t) - X_{VE} \tag{20}$$

In Fig. 15 the extrapolation process is illustrated for the Okoume specimens and the values of X_V and X_{MS} shown in the case of specimen O3.1. The same was done for Padauk and Silver fir. Table 5 shows the results obtained for all specimens. Note that this method disregards the fact that the VE contribution is in reality influenced by MC, that theoretically differs during the sorption cycles.

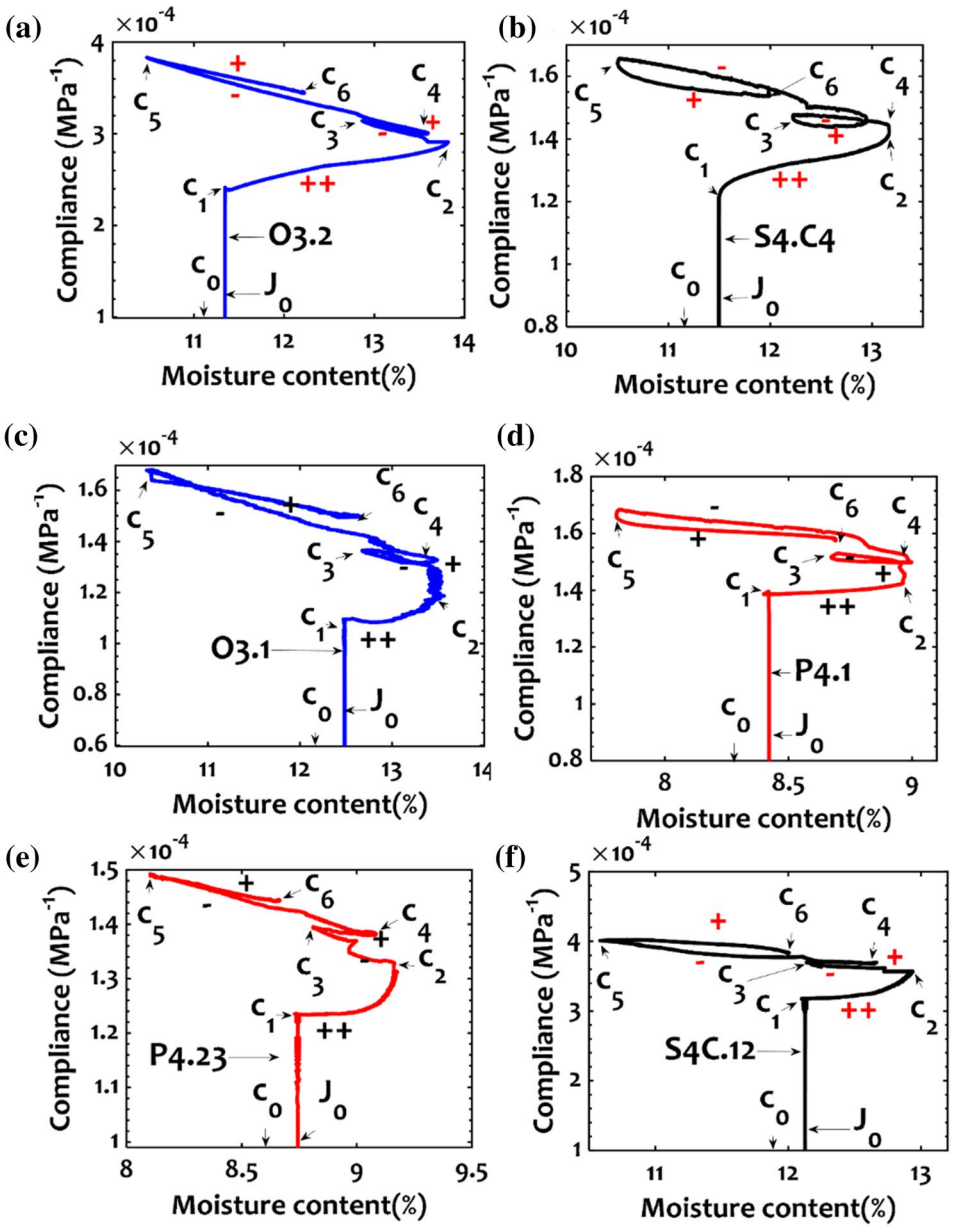

Fig. 14 Trajectories mechano-sorptive (J*) of 14-day test; **a**, **b** test 1 Okoume (O3.2), Silver fir (S4C.4); **c**, **d** test 2 Okoume (O3.1), Padauk (P4.1); **e**, **f** test 3 Padauk (P4.23), Silver fir (S4C.12); (C_1, C_2…C_6 = sorption cycle); J_0 instantaneous compliance

Although the dispersion on J_{vs} and J_{vs} is quite large within each species, there is no evidence of larger viscoelastic creep for the stress level of 35%, although it was performed at a slightly higher humidity level. This finding rather confirms the studies of several authors on viscoelastic linear limit ranging from 35 to 45% of the rupture stress for a bending test (Hoyle et al. 1986; Foudjet 1986; Mukudai 1983). Concerning the mechanosorptive creep, first, the positive X_{MS} values confirm its occurrence. From the higher number of humidity cycles in case of 14-day test, a higher X_{MS} would have been expected, but this was observed only for Okoume. Surprisingly, as shown by Fig. 16, no clear relationship is observed between the contribution to relative creep of mechanosorption and viscoelasticity: Padauk generally exhibited a strong viscoelastic response but little mechanosorption. Its relatively high viscoelasticity could be due to a unusually high MFA, also suggested by the low specific moduli (Table 4). Concerning its small MS, it can be explained by smaller MC variations, these being due to the slower diffusion resulting in a partial effect of RH cycles, and to an unusually small hygroscopicity attributable to specific extractives. In the case of Okoume, on the contrary the two

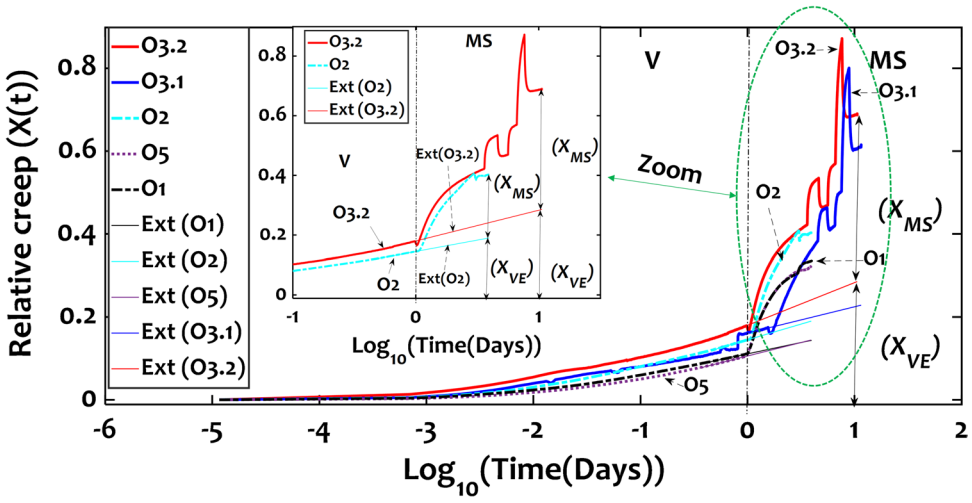

Fig. 15 Separating viscoelastic and mechanosorptive behaviour in the case of Okoume. X_{VE}: viscoelastic contribution obtained by linear extrapolation of 1-day creep; X_{MS} mechanosorptive contribution obtained by difference at the end of the test

Table 5 Relative creep due to viscoelasticity and mechanosorption for each test

Okoume					Padauk				Silver fir		
nb	test	X_{VE}	X_{MS}	nb	test	X_{VE}	X_{MS}	nb	test	X_{VE}	X_{MS}
O3.2	T^{14}_1	0.29	0.40	P4.1	T^{14}_2	0.21	0.08	S4.C4	T^{14}_1	0.20	0.23
O3.1	T^{14}_2	0.19	0.38	P4.23	T^{14}_3	0.28	0.11	S4C.12	T^{14}_3	0.12	0.18
O2	T^{5}_1	0.19	0.21	P1	T^{5}_1	0.40	0.16	S2	T^{5}_1	0.18	0.15
O5	T^{5}_2	0.14	0.17	P3	T^{5}_2	0.25	0.11	S10	T^{5}_2	0.20	0.17
O1	T^{5}_3	0.17	0.19	P6	T^{5}_3	0.19	0.18	S12	T^{5}_3	0.15	0.25
Mean		0.20	0.27			0.27	0.13			0.17	0.20
s.d		0.06	0.11			0.08	0.04			0.03	0.04

X_{VE}: relative viscoelastic creep; X_{MS}: relative mechanocsorptive creep

T^{14}_i: 14-day test at 10% of failure stress; T^{5}_i: 5-day test at 35% of failure stress

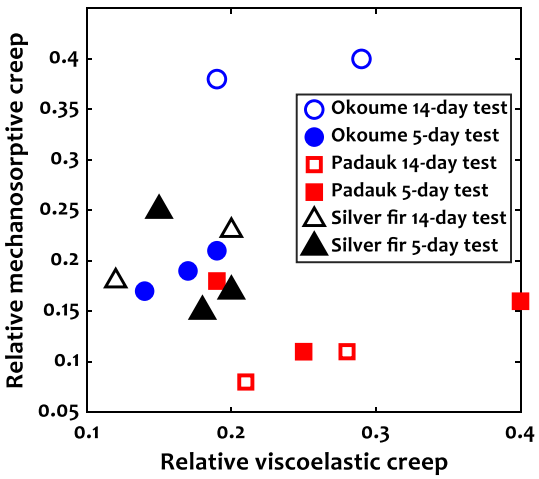

Fig. 16 Relationship between the contribution to relative creep of mechanosorption and viscoelasticity: empty symbols, 14-day tests; filled symbols: 5-day test

specimens from 14-day test expressed a much larger mechanosorption than any other specimen. To evaluate the interaction between viscoelastic and mechanosorptive behaviour, a longer final period at the RH of loading would have been needed to compare the slope to that of the linear extrapolation against *logt*.

In Fig. 17 both contributions to relative creep have been plotted against the specific elastic compliance (ρJ_0, the inverse of the specific Young's modulus) known to be positively correlated with the MFA as recalled above. As expected, a positive trend is observed between the viscoelastic response and ρJ_0 (Fig. 17a): the much higher viscoelastic creep of Padauk could be explained by a higher lower cell-wall rigidity than the specimens of the other species, except Okoume specimen O3.2 also characterised by a high ρJ_0 and high X_{VE}. The trend is not so clear with mechanosorption (Fig. 17b), especially due to the poor contribution of Padauk, possibly due to its high density as suggested above.

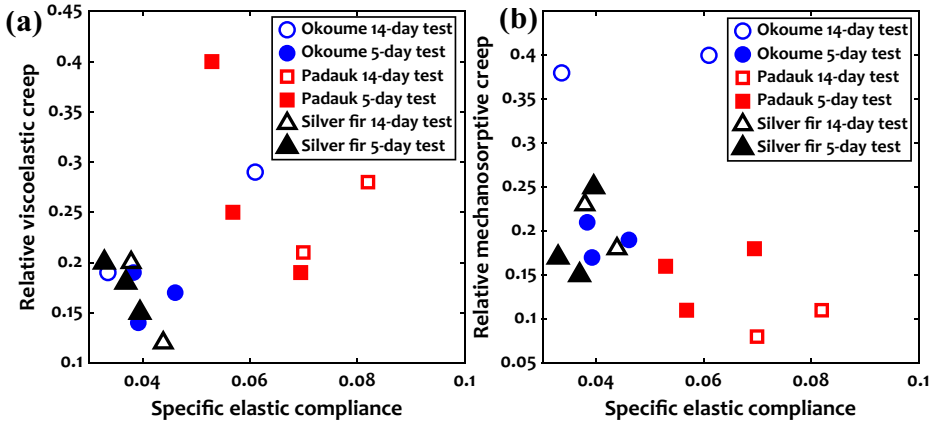

Fig. 17 Relationship between the contribution to relative creep of **a** viscoelasticity and **b** mechanosorption; empty symbols, 14-day test; filled symbols: 5-day test

4 Conclusion

The aim of this work was to study the viscoelastic and mechanosorptive behaviour of two tropical and one temperate species under mechanical loading. Thus, we carried out viscoelastic and mechanosorptive tests on Padauk, Okoume and Silver fir. The specimens were loaded in 3-point bending at 10% and 35% of the rupture stress for 14 days and 5 days under two relative humidity cycling (45, 65 and 75% RH) and (45 and 75% RH). These results also agree with those of several authors, highlighting mechanosorptive and viscoelastic effects at low stress. It was observed that the deformation decreases during the wetting phases, except during the first wetting, and that the drying phases cause an increase in deformation. It was also found that despite its high modulus of elasticity and density, Padauk has higher instantaneous deformation and viscoelastic behaviour than Okoume and Silver fir, but sorption cycles cause less deformation in this species than in the other two. The difference in the level of mechanical (10% and 35% of the rupture stress) and hydric (cycle with moderate and sudden RH variations) loading that we applied to the specimens did not have a significant effect on the viscoelastic behaviour of the wood and tends to confirm that the viscoelastic behaviour remained linear in the two types of tests performed. For this work the mechanosorptive effects were not very pronounced, this is understandable due to the short loading cycles. On the other hand, (++) and (−) effects were observed for the 14-day test. It also appeared that the sorption cycles (wetting and drying) are in favour of an increase in compliance, although the observed behaviour tends to confirm the existence of a limit creep. This work highlighted the viscoelastic and mechanosorptive behaviour of two previously unstudied tropical species and provides an important database for the analysis of the mechanical behaviour of tropical woods, which is not widely available in the literature. The next phase will consist of describing the viscoelastic and mechanosorptive behaviour of the tests carried out with a rheological approach. A similar study will also be carried out on notched specimens to highlight the effects of cracking on the viscoelastic and mechanosorptive behaviour.

Supplementary Information The online version contains supplementary material available at https://doi.org/10.1007/s00107-023-02002-w.

Acknowledgements The authors would like to take this opportunity to thank “le projet CAP 20-25 WOW!” for the financial support provided for the mobility. We also thank the “Hub Innovergne” program for its support.

Authors' contributions All the authors were involved in the manuscript, either directly or indirectly. All authors reviewed and corrected the submitted manuscript. 1–2–4–6 wrote the article and discussed the results. 1–2–3 carried out the experiments with the strong contribution of 1. All the authors participated in the discussion of the results and contributed to the proposal of the experimental protocol.

Funding Not applicable.

Availability of data and materials Not applicable.

Declarations

Conflict of interests The authors declare no competing interests.

Ethical approval Not applicable.

References

Aloisio A, Ussher E, Fragiacomo M, Tomasi R (2023) Capacity models for timber under compression perpendicular to grain with screw reinforcement. Eur J Wood Prod 81:633–654. https://doi.org/10.1007/s00107-022-01918-z

Armstrong LD, Kingston RST (1960) Effect of moisture changes on creep in wood. Nature 185(4716):862–863

Asyraf MRM, Ishak MR, Sapuan SM, Yidris N (2021) Comparison of static and long-term creep behaviors between balau wood and glass fiber reinforced polymer composite for cross-arm application. Fibers Polym 22:793–803. https://doi.org/10.1007/s12221-021-0512-1HUN

Bažant ZP (1985) Constitutive equation of wood at variable humidity and temperature. Wood Sci Technol 19(2):159–177. https://doi.org/10.1007/BF00353077

Brancheriau L, Paradis S (2007) Bing 9-Beam Identification by Non-destructive Grading. CIRAD, Montpellier

Dubois F, Husson JM, Sauvat N, Manfoumbi N (2012) Modeling of the viscoelastic mechano-sorptive behavior in wood. Mech Time-Dependent Mater 16(4):439–460. https://doi.org/10.1007/s11043-012-9171-3

Engonga Edzang AC, Pambou Nziengui CF, Ekomy Ango S, Ikogou S, Moutou Pitti R (2020) Comparative studies of three tropical wood species under compressive cyclic loading and moisture content changes. Wood Mat Sci Eng 16(3):196–203. https://doi.org/10.1080/17480272.2020.1712739

Franke B, Franke S, Schiere MJ (2022) Climate impact on reinforcements in wooden members – effective hygro-expansion coefficients. Wood Mat Sci Eng 17(4):299–308. https://doi.org/10.1080/17480272.2022.2086821

Engelund E, Salmén L (2012) Tensile creep and recovery of Norway spruce influenced by temperature and moisture. Holzforschung 66(8):959–965. https://doi.org/10.1515/hf-2011-0172

Cerre JC, Gérard J, Guibal D, Paradis S. Tropical timber atlas: technological characteristics and uses. Quae. Editions Quae, 2017; 2017–1000.

Gril J. A model of the hygro-rheological behaviour of wood based on its microstructure. PhD Thesis, University Paris 6. In French. 1988.

Gril J. Modelling mechano-sorption in wood through hygro-locks and other approaches. International Symposium on Wood Science and Technology; 2015. https://hal.archives-ouvertes.fr/hal-01295470.

Foudjet A, Bremond C (1989) Creep of four tropical hardwoods from Cameroon. Wood Sci Technol 23:335–341. https://doi.org/10.1007/BF00353249

Grossman PUA, Kingston RST (1954) Creep and stress relaxation in wood during bending. Aust J Appl Sci 5(4):403–417

Grossman PUA (1971) Use of Leicester's rheological model for mechano-sorptive deflections of beams. Wood Sci Technol 5(3):232–235. https://doi.org/10.1007/BF00353685

Hamdi SE, Pitti RM, Gril J. Moisture driven damage growth in wood material: 3D image analysis for viscoelastic numerical model validation, WCTE 2018 - World Conference on Timber Engineering. 2018.

Hanhijärvi A, Hunt D (1998) Experimental indication of interaction between viscoelastic and mechano-sorptive creep. Wood Sci Technol 32(1):57–70. https://doi.org/10.1007/bf00702560

Hou J, Jiang Y, Yin Y, Zhang W, Chen H, Yu Y, Jiang Z (2021) Experimental study and comparative numerical modeling of creep behavior of white oak wood with various distributions of earlywood vessel belt. J Wood Sci 67:1–13

Houanou AK, Tchéhouali AD, Foudjet AE (2014) Effect of the loading duration on the linear viscoelastic parameters of tropical wood: Case of Tectona grandis Lf (Teak) and Diospyros mespiliformis (Ebony) of Benin Republic. Springer 3(1):1–12. https://doi.org/10.1186/2193-1801-3-74

Hoyle R, Itani R, Eckard J (1986) Creep of Douglas fir beams due to cyclic humidity fluctuations. Wood Fiber Sci 18(3):468–477

Hunt, D.G. (1984). Creep trajectories for beech during moisture changes under load. J Mater Sci 19, 1456–1467.https://doi.org/10.1007/BF00563040

Hunt DG (1989) Linearity and non-linearity in mechano-sorptive creep of softwood in compression and bending. Wood Sci Technol 23(4):323–333. https://doi.org/10.1007/BF00353248

Hunt DG (2004) The prediction of long-time viscoelastic creep from short-time data. Wood Sci Technol 38(7):479–492. https://doi.org/10.1007/s00226-004-0244-6

Hunt DG (1986) The mechano-sorptive creep susceptibility of two softwoods and its relation to some other materials properties. J Mater Sci 21:2088–2096. https://doi.org/10.1007/BF00547951

Hunt DG. Present knowledge of mechano-sorptive creep of wood. RILEM Report, p. 73–97; 1994.

Llana DF, Hermoso E, Bobadilla I, Iñiguez-Gonzalez G (2018) Influence of moisture content on the results of penetration and withdrawal resistance measurements on softwoods. Holzforschung 72(7):549–555. https://doi.org/10.1515/hf-2017-0133

Manfoumbi Boussougou N, Pambou Nziengui CF, Moutou PR (2022) Creep behaviour of timber structures in variable tropical climates: Application to Dacryodes buettneri and baillonella toxisperma species. Constr Build Mater 344:128284. https://doi.org/10.1016/j.conbuildmat.2022.128284

Mohager S, Toratti T (1992) Long term bending creep of wood in cyclic relative humidity. Wood Sci Technol 27(1):49–59. https://doi.org/10.1007/BF00203409

Montero C, Gril J, Legeas C, Hunt DG, Clair B (2012) Influence of hygromechanical history on the longitudinal mechanosorptive creep of wood. Holzforschung 66(6):757–764. https://doi.org/10.1515/hf-2011-0174

Mukudai J (1983) Evaluation of linear and non-linear viscoelastic bending loads of wood as a function of prescribed deflections. Wood Sci Technol 17(3):203–216. https://doi.org/10.1007/BF00372319

Mukudai J, Yata S (1987) Further modeling and simulation of viscoelastic behavior (bending deflection) of wood under moisture change. Wood Sci Technol 21(1):49–63. https://doi.org/10.1007/BF00349717

Navi P, Pittet V, Plummer CJG (2002) Transient moisture effects on wood creep. Wood Sci Technol 36(6):447–462. https://doi.org/10.1007/s00226-002-0157-1

Navi P, Heger F. Thermo-hydro-mechanical behaviour of wood: technical and structural applications. First edition, Presses Polytechniques et Universitaires Romandes, Lausanne, CH, p. 119–120. In french. 2005.

Nguyen SL, Saifouni O, Destrebecq JF. Incremental Formulation for Coupled Viscoelasticity and Hydrolock Effect in Softwood. In: Ralph C, Silberstein M, Thakre P, Singh R (eds). Mechanics of Composite and Multi-functional Materials, Conference Proceedings of the Society for Experimental Mechanics Series. Springer: Cham; 2016.

Nkene Mezui E, Pambou Nziengui CF, Moutou Pitti R, Ikogou S, Ekomy Ango S, Talla PK (2023) Strain and cracks investigations on tropical green wood slices under natural drying: experimental and numerical approaches. Eur J Wood Prod 81(1):187–207. https://doi.org/10.1007/s00107-022-01881-9

O'Ceallaigh C, Sikora K, McPolin D, Harte AM (2020) Modelling the hygro-mechanical creep behaviour of FRP reinforced timber elements. Constr Build Mater 259:119899

Peng H, Jiang J, Lu J, Cao J (2019) Orthotropic mechano-sorptive creep behavior of Chinese fir during the moisture adsorption process determined in tensile mode via dynamic mechanical analysis (DMA). Holzforschung 73(3):229–239. https://doi.org/10.1515/hf-2018-0067

Pittet V. Experimental study of mechanosorptive couplings in wood subjected to controlled hygrometric variations under long-term loading. PhD thesis, Ecole Polytechnique de Lausanne, Switzerland. 1996. **(In French)**

Placet V. Design and operation of an innovative experimental device for the characterization of the viscoelastic behaviour and thermal degradation of wood under severe conditions. To cite this version : HAL Id : tel-00116612 PhD thesis , University Henri Poincaré - Nancy I. In French; 2006.

Ratanawilai T, Srivabut C (2022) Physico-mechanical properties and long-term creep behavior of wood-plastic composites for construction materials: effect of water immersion times. Case Stud Constr Mater 16:e00791

Ranta-Maunus A (1975) The viscoelasticity of wood at varying moisture content. Wood Sci Technol 9:189–205. https://doi.org/10.1007/BF00364637

Randriambololona H, Dubois F, Petit C (2002) Modelling the deferred mechanical behaviour of wood in a variable environment. French J Civil Eng 6(7–8):1333–1357. https://doi.org/10.1080/12795119.2002.9692412.InFrench

Saifouni O, Destrebecq JF, Froidevaux J, Navi P (2016) Experimental study of the mechanosorptive behaviour of softwood in relaxation. Wood Sci Technol 50(4):789–805. https://doi.org/10.1007/s00226-016-0816-2